EO-1 HYPERION MEASURES CANOPY DROUGHT STRESS IN AMAZÔNIA

Gregory P. Asner,[1] Daniel Nepstad,[2,3] Gina Cardinot,[2]
Paulo Moutinho,[2] Thomas Harris,[1] David Ray[3]

1. Introduction

Amazon moist tropical forests account for about 70–80 Pg (70–80 x 10^{15} g) of the world's terrestrial carbon stocks and roughly 4–6 Pg (~10%) of the annual net primary productivity (NPP). Because of the large carbon pools and fluxes in this region, much attention has focused on the effects of land use on Amazon forest cover and carbon storage, and on the potential feedbacks to regional and global climate (Shukla et al. 1990). The role of climate in modulating interannual variability of Amazon forest phenology and NPP has received little attention until recently (Tian et al. 1998, Asner et al. 2000), yet this variation may be significant from both climatological and ecological perspectives. Large uncertainties persist regarding spatial and temporal patterns of biosphere-atmosphere carbon exchange, and these uncertainties impede global analyses of CO_2 sources and sinks, and thus changes in climate forcing (Ciais et al. 1995). Climate-driven phenology and NPP variability in the Amazon also has important implications for basin hydrology, river biology and biogeochemistry, trace gas fluxes, and spatial and temporal patterns of land-use change.

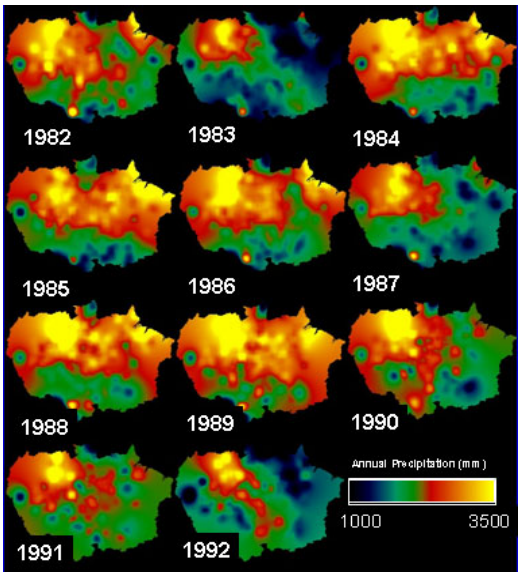

Figure 1. Interannual precipitation variability in the Amazon basin. ENSO periods (1983, 1987, 1991-1992) can be linked to decreased rainfall, especially in the southeast region of the basin (Asner et al. 2000)

There is now increasing focus on the effects of the El Niño-Southern Oscillation (ENSO), which is known to decrease rainfall in the Amazon basin (Marengo 1992). For example, the 1983, 1987, and 1991/92 ENSO events varied in strength, but all resulted in anomalously low precipitation throughout much of the region (Figure 1). Because the factors controlling forest phenology and productivity throughout the tropics are not well known, independent observations are needed to evaluate estimates of a biological response to climate variation.

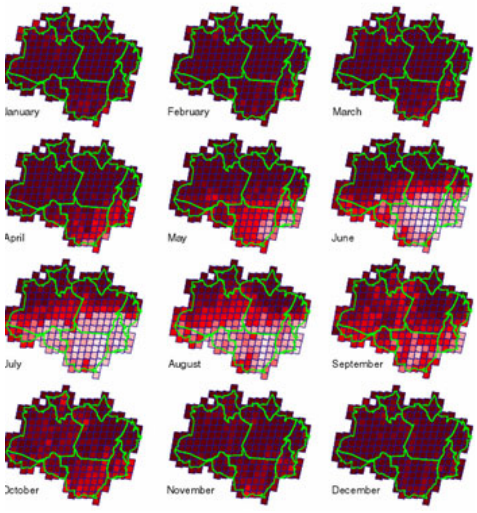

Figure 2. Cloud cover probability by month for Landsat imagery of the Brazilian Amazon (Asner 2001). Whiter indicates fewer clouds.

Whereas annual variations in rainfall are starting to be understood in the Amazon Basin, seasonal variations are not well known. There is a pronounced dry season that extends from June to November throughout the eastern and central Amazon, but spatial variation in the strength of this dry season remains poorly quantified. Phenological losses of canopy foliage are reduced during the dry season through forest deep root access to soil water reserves (Nepstad et al. 1994). Nonetheless, field measurements do show that Amazon forest canopies respond to seasonal dry periods, with litterfall increases of 10–35% and decreases of total leaf area index (LAI) of up to 30% (Asner et al. 2000, Nepstad et al. 2002). Cloud cover information from more than 54,000 Landsat images of the Brazilian Amazon yielded a spatial proxy for seasonal rainfall patterns in the Amazon, as shown in Figure 2.

[1] Carnegie Institution of Washington, Stanford California
[2] Instituto de Pesquisa Ambiental da Amazônia, Bélem, Brazil
[3] The Woods Hole Research Center, Woods Hole, Massachusetts

The central, south and southeast portions of the Amazon Basin experience a period of decreased cloud cover and precipitation from June through November.

There are likely important effects of seasonal and interannual rainfall variation on forest leaf area index, canopy water stress, productivity and regional carbon cycling in the Amazon. While both ground and spaceborne studies of precipitation continue to improve, there has been almost no progress made in observing forest canopy responses to rainfall variability in the humid tropics. This shortfall stems from the large stature of the vegetation and great spatial extent of tropical forests, both of which strongly impede field studies of forest responses to water availability. Those few studies employing satellite measures of canopy responses to seasonal and interannual drought (e.g., Bohlman et al. 1998, Asner et al. 2000) have been limited by the spectral resolution and sampling available from Landsat and AVHRR sensors.

We report on a study combining the first landscape-level, managed drought experiment in Amazon tropical forest with the first spaceborne imaging spectrometer observations of this experimental area. Using extensive field data on rainfall inputs, soil water content, and both leaf and canopy responses, we test the hypothesis that spectroscopic signatures unique to hyperspectral observations can be used to quantify relative differences in canopy stress resulting from water availability.

2. Study Region and Areas

The experiment was located in Brazil's Tapajós National Forest, in east-central Amazonia (2.897º S, 54.952ºW; Figure 3). This forest receives 600–3000 mm of rain each year, with a mean of 2000 mm; it experiences severe drought during El Niño events (Figure 1). The forest is situated on a flat terrace of Tertiary sediments capped by the Belterra Clay Formation, and is approximately 90 m above the water level of the Tapajós River, located 10 km to the west. The Oxisol soil (Haplustox) is dominated by kaolinite clay minerals and is free of hardpan or iron oxide concretions in the upper 12 m. The water table is located at ~100 m depth.

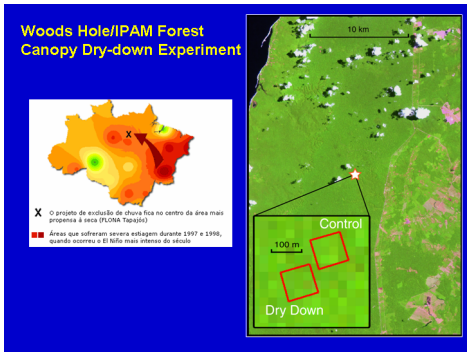

Figure 3. (left) Location of forest drought experiment in the central Brazilian Amazon. (right) Landsat image of forest drought experiment and control area, located within the Tapajos National Forest.

We selected two floristically and structurally similar, one-ha (100 x 100 m) plots from an initial survey of 20 hectares of forest. We encountered 182 and 203 species represented by individuals with diameter at breast height (1.3 m, dbh) of at least 10 cm (trees) and 5 cm (lianas) in the treatment and control plots, respectively. The plots shared 54 tree species in common with at least 2 individuals per plot, therefore allowing us to compare responses to the experimental treatment within the same species. The plots also had similar physiognomy, with the exception of a 600-m^2 treefall gap on the edge of the control plot. The forest surrounding the plots had emergent trees up to 55 m in height, with continuous canopy varying in height from 18 to 40 m. The study plots were placed in areas where most of the canopy was <30 m high to facilitate access to the tree crowns. Above-ground biomass of trees =10 cm dbh and lianas =5 cm basal diameter at the beginning of the experiment was 291 and 305 Mg ha-1 in the treatment and control plots, respectively.

At their closest points, the plots were 25 m apart. Four wooden towers (13-30 m in height) and 80-100 m of catwalk (8-12 m height) provided access to the canopy in each of the 1-ha plots. Soil shafts (12-m deep, with 2.1 x 0.8 m openings, n=3 per plot and n=5 as of April 9, 2001), with a wooden infrastructure, provided belowground access. Sampling grids with 10-m distances between points were established with 10 x 10 points inside of each plot and a perimeter of sampling points outside of each plot, for a total of 12 x 12 = 144 points. These grids were used for measurements of surface soil water content, leaf area index, canopy openness, and other measures. A 1- to 1.7-m deep trench was excavated around the treatment plot to reduce the potential for lateral movement of soil water from the surrounding forest into the plot, and to provide a conduit for water excluded from the plot. A similar trench was excavated around the control plot to avoid the confounding of throughfall exclusion and trenching effects. As with many large-scale ecosystem manipulations, this experiment was prohibitively large and expensive to permit replication.

Throughfall was partially excluded from the treatment plot during the rainy season of 2000, from late January through early August, and during the rainy season of 2001, from early January through late May, using 5,660 panels made of clear, PAR-transmitting greenhouse plastic mounted on wooden frames. The panels were removed during the dry season to reduce their influence on the forest floor through shading and heating. The panels

increased forest floor temperature by no more than 0.3°C. While they were in place, the panels were flipped on their sides every two to three days to transfer accumulated litter onto the forest floor. Each 3 x 0.5 m panel drained into a plastic-lined, wooden gutter (30 cm wide) that carried the water into the trench, which was also lined with plastic. Water flowed by gravity from the perimeter trench into a deeper drainage ditch (1.7–2.3 m depth), which extended 220 m away from the plot into a small valley. The panels and gutters covered only ~75% of the forest floor, because openings we left around tree stems. We did not exclude stemflow from the plot. Estimates of daily rainfall were made with two wedge-shaped rain gauges located in the center of an 80-m wide clearing 500 m from the experimental plots. Trampling of the forest floor was reduced in the experimental plots by directing foot traffic onto wooden walkways. Despite this precaution, 17% of the treatment plot and 15% of the control plot had visible signs of foot traffic as of January, 2001 (based on three, randomly-placed, 100-m transects across each plot). Forest floor damage in the treatment plot was greater than in the control plot because of the installation of panels and gutters. However, the control plot suffered similar forest floor damage because measurements of canopy cover, leaf area index, litterfall, and throughfall within the sampling grid required ground access; elevated drainage gutters provided access to the grid in the treatment plot.

3. Field Sampling

The amount of throughfall excluded by the panels was calculated for each exclusion period as the increase in soil water content in the control plot minus the increase in soil water content in the treatment plot, plus the difference between deep seepage of soil water (below 11 m depth) in the control and treatment plots. Deep seepage was estimated as evapotranspiration minus rainfall minus the increase in soil water content for a given time interval. Evapotranspiration was assumed to be 4 mm per day, based on published estimates for Amazon forest ET during the wet season. Drought affects forests primarily through its effects on soil moisture. Previous studies have found that forests in seasonally-dry Amazonia absorb soil water from depths of 8 m and more during periods of severe drought (Nepstad et al. 1994). We therefore monitored volumetric soil water content (cm^3 water cm^{-3} soil) to 11 m depth in both the treatment and control plots.

We measured soil water using Time Domain Reflectometry (TDR) to a soil depth of 30 cm. The pre-dawn leaf water potential of mature trees was measured at approximately 2-wk intervals during the dry seasons and at longer time intervals during the wet seasons to provide a measure of canopy drought stress. Six tree species common to both forest plots were studied, with three individuals per species in each plot, and four leaves sampled per individual. Leaves were clipped before sunrise, and stored in plastic bags on ice until water potential was measured using a pressure chamber. Measurements were always completed within one hour of clipping.

We measured leaf area index (LAI) before and during the throughfall exclusion treatment at each of the grid sampling points using LICOR LAI-2000 Plant Canopy Analyzers. One instrument was placed above the canopy on a tower to measure incoming radiation with no canopy influence; the other instrument was used for the understory measurement, made with the same directional orientation as the above-canopy instrument. The instruments were inter-calibrated above the canopy at the beginning of each set of measurements. Measurements were made under conditions of diffuse skylight. LAI calculations were made using the inner three quantum sensor rings to minimize the overlap among measurements made in adjacent grid points.

4. Spaceborne Imaging Spectroscopy

Earth Observing-1 (EO-1) Hyperion imaging spectrometer data were collected over the experimental sites in July and November 2001, corresponding with the early and late parts of the dry season. Details of the mission are available on the EO-1 internet website at: http://eo1.gsfc.nasa.gov. The imagery was delivered in L1A calibrated radiance format from NASA Goddard Space Flight Center (GSFC), Greenbelt, Maryland. Three calibration steps were applied to the radiance as suggested by GSFC: (1) a pixel shift was applied to samples 129–256 in the shortwave-infrared (SWIR) wavelength region to co-register this portion of the data with the visible and near-infrared (NIR) observations; (2) the visible and NIR bands were multiplied by a scale factor of 1.08, and the SWIR bands were multiplied by a scale factor of 1.18; and (3) the wavelength values were increased by 2 nm for all bands. These steps were necessary to bring the data set up to the currently available calibration level. The Hyperion data were then spectrally and spatially subset. The zero-value visible bands 1–4 and SWIR bands 226–242 and the overlapping bands 58–78 were removed, resulting in a 200 band subset.

Apparent surface reflectance was estimated from the Hyperion radiance data using the ACORN atmospheric correction algorithm (AIG-LLC, Boulder, Colorado). ACORN uses the 1.14 μm water vapor feature to compute atmospheric water vapor thickness. The water vapor bands near 1.4 and 1.8 μm were then removed. The

resulting reflectance spectra still contained some anomalies; however, no ground calibration was applied since the noise was not systematic.

The two calibrated spectral reflectance cubes were geo-located using differentially-corrected GPS data points collected throughout the area. Owing to the fact that all calibration steps, including atmospheric correction, are not perfect, and given our interest in isolating relatively small differences in canopy reflectance between the two sites, we employed a comparative analysis of the sites by ratioing spectral signatures. Since the two sites were close together spatially, site-based ratioing of the results eliminated the contribution of atmospheric differences to the multi-date comparison of sites.

5. Spectroscopic Indices

Imaging spectroscopy offers a unique set of observations – and thus tools – to analyze the molecular absorption and scattering features of materials. Traditional multi-spectral observations, such as from Landsat, SPOT, AVHRR and MODIS sensors, provide a subset of the capabilities provided by hyperspectral imagers. Although imaging spectroscopy affords the means to analyze full spectral features of materials, many vegetation indices have been developed to condense and simplify the analysis of high-dimensional spectral data while also attempting to maximize the information content of the indices. The normalized difference vegetation index (NDVI) is a prime example. The NDVI is the normalized difference of reflectance at red (~680 nm) and near-infrared (~750–850 nm) wavelengths (= [NIR-RED]/[NIR+RED]). The NDVI is sensitive to canopy greenness, fractional photosynthetic radiation absorption (fPAR) and canopy leaf area. It is available from nearly all multi-spectral sensors. However, the NDVI is also known to become insensitive, or to saturate, in canopies with leaf area indices (LAI) greater than about three or four (Choudhury 1987, and many others).

Novel vegetation indices have been developed using imaging spectrometers. These indices are derived from a variety of spectral channels, often using observations from very narrow wavelength regions of the spectrum. Because leaf pigments absorb photons at visible wavelengths (400-690 nm), whereas water absorbs in near-IR (750–1300 nm) and shortwave-IR (1500–2500 nm) regions, a narrow and contiguous sampling of the spectrum at these wavelengths allows the development highly sensitive indices. The following are a few indices that have proven useful to understanding the spatial and temporal dynamics of vegetation:

Table 1. Five narrowband vegetation indices available for analysis from the EO-1 Hyperion spaceborne imaging spectrometer.

Index	Index Name	Equation	Reference
NDVI	Normalized Difference Vegetation Index	(R800-R680)/(R800+R680)	Choudhury (1987)
SR	Simple Ratio	R800/R680	Sellers (1985)
NDWI	Normalized Difference Water Index	(R857-R1241)/(R857+R1241)	Gao (1996)
PRI	Photochemical Reflectance Index	(R531-R570)/(R531+R570)	Gamon et al. (1992)
ARI	Anthocyanin Reflectance Index	(1/R550) – (1/R700)	Gitelson et al. (2001)

The simple ratio (SR) is one of the oldest vegetation indices. Like the NDVI, it is sensitive to canopy greenness, fPAR and leaf area. The normalized difference water index (NDWI) was designed for sensitivity to canopy water content (Gao 1996). Two pigment-related indices unique to imaging spectroscopy are the photochemical reflectance index (PRI; Gamon et al. 1992) and anthocyanin reflectance index (ARI; Gitelson et al. 2001). The PRI has been used to study changes in xanthophyll cycle pigments, providing a means to estimate photosynthetic light-use efficiency (LUE). Anthocyanins are water soluble pigments that cause the red coloration of plant tissues. These red pigments are expressed differentially by species and within species, with observed variations resulting from leaf aging, stress and nutrient status.

We used the EO-1 Hyperion spectrometer observations to calculate these five narrow-band vegetation indices. We ratioed the sites to look for differences that might be the result of precipitation throughfall exclusion in the Amazon forest dry-down experiment.

6. Results and Discussion

Differences in plant available water (PAW) in the soils of the drydown and control forest areas were pronounced (Figure 4). In comparison to the control area, PAW was 54% and 56% lower in the drydown site in July and November, respectively. Decreasing PAW followed the well-known monthly pattern of decreasing rainfall during the dry season (June–December), but the precipitation throughfall exclusion greatly enhanced the effect of seasonal drought on the drydown forest area (Figure 4).

The average canopy reflectance spectra from EO-1 Hyperion of the dry-down and control areas are shown in Figure 5. A zoom graph of the visible (500–700 nm) spectral range and the spectral bands used to create the narrow-band vegetation indices is also provided. Visible reflectances were higher and near-IR reflectances were lower in the early dry-season (July) in comparison to the late dry-season (November). These differences between imaging dates likely resulted from changes in upper-canopy architecture, canopy water content, and LAI; however, a precise cause for this observed change is not clear. It is also possible that these general differences in the visible and near-IR spectral regions are due to atmospheric effects.

Both canopies maintained LAI values in July and November, and these LAI values were well into the saturation zone for both the NDVI and SR (Figures 6). The LAI of the control area actually increased from July to November, while it decreased slightly in the drydown site. Leaf water of the drydown and control canopies was also similar in July and November (Figure 6).

Despite the similarity of LAI and leaf water within each site at the beginning and end of the dry season, there were substantial differences between the two sites on each imaging date. The drydown site had an average LAI value that was 8% and 19% lower than the control area in July and November, respectively (Figure 6). While leaf water was nearly the same in the drydown and control sites in July, the drydown area was nearly 30% lower in leaf water at the end of the dry season (November).

Another important biophysical difference between the drydown and control areas was found in the specific leaf area (SLA) values of species common to both sites. SLA is the leaf area per unit mass, which is a good inter-species indicator of leaf thickness. SLA values were nearly twice a high among species in the control than in the drydown forest areas (Figure 7). This finding indicated that the vegetation responded to persistent drought by developing leaves of greater thickness, which reduced transpiration and increased leaf longevity.

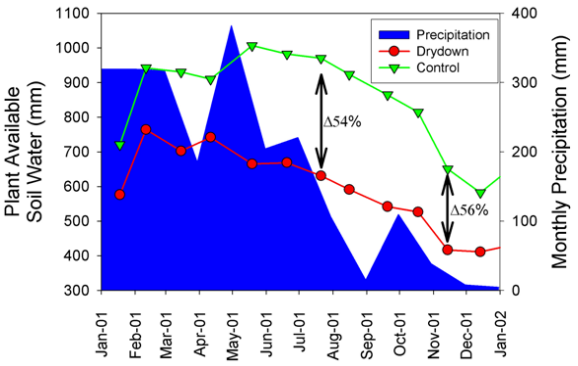

Figure 4. Monthly plant available soil water (mm) and precipitation for the period January 2001–2002. EO-1 Hyperion acquisition dates are shown in black arrows.

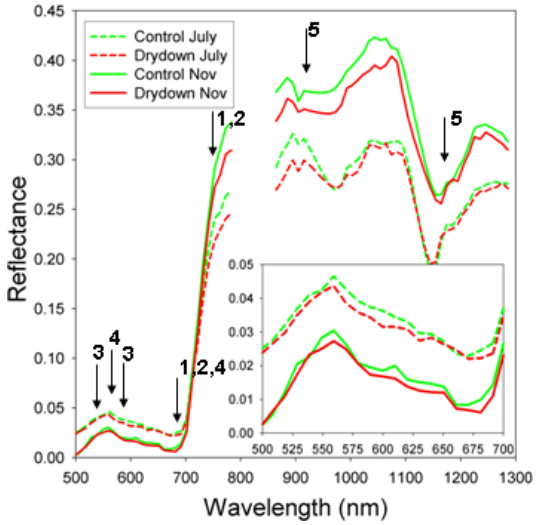

Figure 5. Hyperspectral reflectance signatures of control and drydown sites in the Central Amazon, acquired in July and November 2001 by EO-1 Hyperion. Numbers show spectral bands used to calculate the (1) NDVI, (2) SR, (3) PRI, (4) ARI, and (5) NDWI.

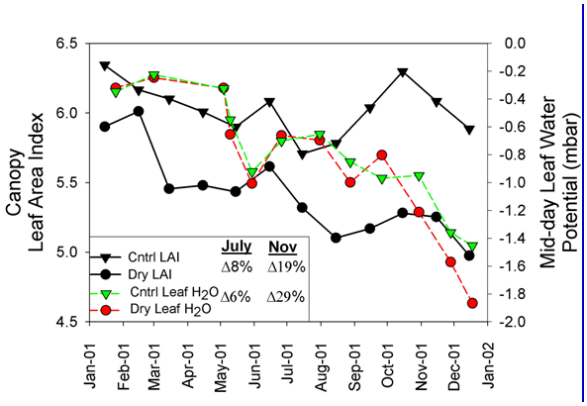

Figure 6. Monthly LAI and mid-day leaf water potential from January 2001-2002 for the control and drydown experimental areas. Percentage differences in LAI and leaf water at each Hyperion observation date are shown in the legend.

A summary of all major leaf and canopy properties for the drydown and control forest areas in July and November 2001 is provided in Table 1. In July at the beginning of the dry season, plant available soil water and leaf water potential were both high in the control area but decreased to moderate levels by the end of the dry season in November. During both imaging periods, LAI and leaf thickness (1/SLA) were very high and low, respectively, in the control area.

In contrast to the control area, the drydown forest site had moderate plant available soil water and high leaf water in July. Both of these properties decreased dramatically to low levels by November. Meanwhile, both LAI and leaf thickness (1/SLA) remained high at the beginning and end of the dry season in 2001 (Table 2).

These differences between drydown and control forest areas, at the start and end of the dry season, had differential effects on the hyperspectral narrowband indices derived from the EO-1 Hyperion imagery (Figure 8). Interestingly, the ratio of NDVI and SR values for the drydown and control areas remained nearly constant at 1.0 in both July and November. This indicated no measurable NDVI or SR response of the drought either at the beginning or end of the dry season. This result is not surprising, given that the NDVI and SR saturate at LAI values in the three to four range. This result suggests that multi-spectral sensors, such at Landsat or AVHRR, cannot detect changes in canopy "greenness" as provided by the NDVI or SR for drought conditions in Amazon humid tropical forests.

In contrast to the traditional NDVI and SR indices, the canopy water index (NDWI) was highly sensitive to drought conditions (Figure 8). The ratio of drydown:control area NDWI was nearly 1.0 (no difference) at the beginning of the dry season (July) but decreased substantially to about 0.25 by the end of the dry season in November.

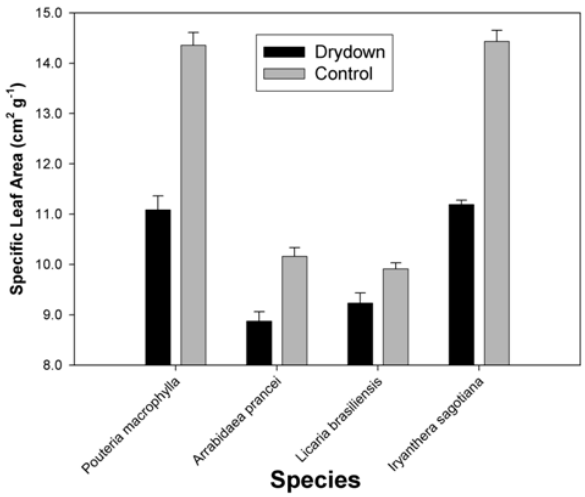

Figure 7. Specific leaf area – a measure of leaf thickness – for four species common to the drydown and control forest areas.

Canopy Properties and Changes During Dry Season

Control Forest	*July*	*November*
Plant-avail Water	High	Moderate
Leaf Water	High	Moderate
LAI	Very High	Very High
Leaf Thickness	Low	Low
Drydown Forest		
Plant-avail Water	Moderate	Low
Leaf Water	High	Low
LAI	High	High
Leaf Thickness	High	High

Table 2. Summary of leaf and canopy properties in the control and drydown forest areas in July and November 2001.

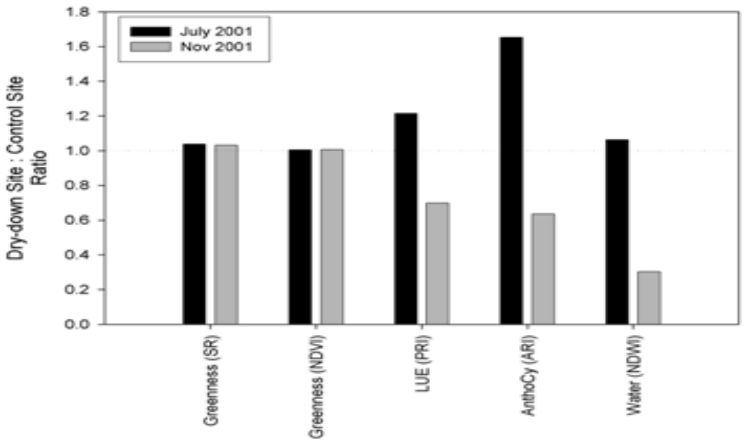

Figure 8. Ratio of narrowband vegetation indices for drydown vs. control areas, derived from EO-1 Hyperion in July and November, 2001.

This result suggests that the NDWI is sensitive to canopy foliage area and water content at high values obtained by tropical forests. This also indicates that the effects of the precipitation throughfall exclusion were best observed at the end of the dry season, when the affects of drought are at maximum. These effects were most evident in the plant available soil water, leaf water and leaf thickness data obtained in the field (Table 2).

Light-use efficiency (LUE), or the amount of carbon uptake by vegetation per unit energy absorption, is a critically important determinant of net primary production in ecosystems (Field et al. 1995). Hyperion observations indicated about a 20% higher and a 20% lower LUE in the drydown area in July and November, respectively (Figure 8). It is difficult to ascertain the cause of increased LUE in the drought-stressed forest at the beginning of the dry season. It is possible that this site had a flush of new foliage prior to the July image, a potential response to foliage loss in the previous dry season. This hypothesis is supported by the concomitant observation of 60% higher anthocyanin levels (ARI; Table 1) in the drydown site at the beginning of the dry season. Anthocyanin, or leaf redness, is a general indicator of newly-formed foliage prior to the full development of chlorophyll pigments that changes the leaf color to green. The much lower LUE in the drydown (vs. control) by the end of the dry season is more understandable, as the drought site had much less leaf water at this time of the year. A simultaneous indicator of anthocyanin levels (ARI) showed 40% lower values in the drydown as compared to the control area in November.

7. Conclusions

The results presented in this communication indicate that narrowband vegetation indices available from the spaceborne imaging spectrometer, EO-1 Hyperion, can be used to monitor drought impacts on humid tropical forests. The first-ever measurements of soil and plant water stress at the landscape scale were combined with the first-ever spaceborne imaging spectrometer observations to test the sensitivity of these hyperspectral indices. We found that:

a. Drought stress in the central Amazon is most evident in decreased plant available soil water, leaf water potential, and specific leaf area.
b. Narrowband NDVI and SR observations are insensitive to changes in leaf area index and canopy water content in humid tropical forests.
c. Narrowband canopy water observations (NDWI) are highly sensitive the changes in canopy leaf area and water content in humid tropical forests.
d. Narrowband pigment indices related to light-use efficiency and anthocyanin levels indicate the onset of stress effects caused by chronic water stress.

These preliminary findings strongly suggest that only narrowband, hyperspectral observations can be used to detect canopy drought stress in humid tropical forests such as in the central Amazon Basin. Additional spaceborne imaging spectrometer observations are critically needed to continue this assessment in other forest types and climatic conditions.

8. Acknowledgements

This work was supported by NASA NIP grant NAG5-8709, NASA New Millenium (EO-1) Program grant NCC5-481, and the National Science Foundation.

9. References

Asner, G.P., Cloud cover in Landsat observations of the Brazilian Amazon, *International Journal of Remote Sensing*, 22, 3855–3862, 2001.

Asner, G.P., A.R. Townsend, and B.H. Braswell, Satellite observation of El Niño effects on Amazon forest phenology and productivity, *Geophysical Research Letters*, 27, 981–984, 2000.

Bohlman, S.A., J.B. Adams, D.L. Peterson, Seasonal foliage changes in the Eastern Amazon Basin detected from Landsat Thematic Mapper satellite images, *Biotropica*, 30, 376–393, 1998.

Choudhury, B.J., Relationships between vegetation indices, radiation absorption and net photosynthesis evaluated by a sensitivity analysis, *Remote Sensing of Environment*, 22, 209–233, 1987.

Ciais, P., et al., A large northern hemisphere CO_2 sink indicated by the $^{13}C/^{12}C$ ratio of atmospheric CO_2, *Science*, 269, 1098–1102, 1995.

Field, C.B., et al., Global net primary production: combining ecology and remote sensing, *Remote Sensing of Environment*, 51, 74–88, 1995.

Gamon, J.A., J. Penuelas, and C.B. Field, A narrow-waveband spectral index that tracks diurnal changes in photosynthetic efficiency, *Remote Sensing of Environment*, 41, 35–44, 1992.

Gao, B.-C., and A.F.H. Goetz, Retrieval of equivalent water thickness and information related to biochemical components of vegetation canopies from AVIRIS data, *Remote Sensing of Environment*, 52, 155–162, 1995.

Gitelson, A.A., M.N. Merzlyak, and O.B. Chivkunova, Optical properties and nondestructive estimation of anthocyanin content in plant leaves, *Photochemistry and Photobiology*, 74, 38–45, 2001.

Marengo, J.A., Interannual variability of surface climate in the Amazon basin, *International Journal of Climatology*, 12, 853–863, 1992.

Nepstad, D., et al., The role of deep roots in the hydrological and carbon cycles of Amazonian forests and pastures, *Nature*, 372, 666–669, 1994.

Nepstad, D., et al. The effects of partial throughfall exclusion on canopy processes, aboveground production, and biogeochemistry of an Amazon forest, *Journal of Geophysical Research*, 2002.

Sellers, P.J. Canopy reflectance, photosynthesis, and transpiration, *International Journal of Remote Sensing*, 6, 1335–1372, 1985.

Shukla, J., et al., Amazon deforestation and climate change, *Science*, 247, 1322-1325, 1990.

Tian, H., et al., Effect of interannual climate variability on carbon storage in Amazonian ecosystems, *Nature*, 396, 664–667, 1998.